Tectonics®

RESEARCH ARTICLE
10.1029/2025TC009070

Morphometric Evidence for Cenozoic Intraplate Reactivation in NW Uruguay

Mauricio B. Haag[1,2], Lindsay M. Schoenbohm[1,2], Rossano Dalla Lana Michel[3], Claiton M. dos Santos Scherer[3], Gerardo Veroslavsky[4], and Josefina Marmisolle[5,6]

[1]Department of Earth Sciences, University of Toronto, Toronto, ON, Canada, [2]Department of Chemical and Physical Sciences, University of Toronto Mississauga, Mississauga, ON, Canada, [3]Instituto de Geociências, Universidade Federal do Rio Grande do Sul, Porto Alegre, Brazil, [4]Facultad de Ciencias, Universidad de la República, Montevideo, Uruguay, [5]PEDECIBA Geociencias, Universidad de la República, Montevideo, Uruguay, [6]Transición Energética, ANCAP, Montevideo, Uruguay

Abstract Located in eastern South America, Uruguay has been considered tectonically inactive since rifting in the Late Cretaceous. Here, we use a high-resolution digital elevation model and field observations to investigate the presence of recent tectonic activity in the Basaltic Plateau, northwest Uruguay. Based on topographic, drainage network and field-based data, we identify evidence for long-lasting, and potentially Quaternary tectonic deformation, including fault breccia, scarps, and offset channels, suggesting strike-slip and normal faulting. The orientation and spatial pattern of this deformation aligns closely with inherited structures, particularly Proterozoic and Mesozoic fault zones. Our results suggest that reactivation of ancient basement structures has localized recent deformation, highlighting the importance of tectonic inheritance in controlling deformation in intraplate regions, considered otherwise tectonically "inactive." The detection of subtle, recent deformation in Uruguay is only possible because of high-resolution topographic data, underscoring the role of modern remote sensing tools in assessing tectonic activity in presumed stable regions. Lastly, this study highlights the need to reassess intraplate landscapes for signs of recent deformation, particularly in regions underlain by major basement structures that may act as zones of weakness, facilitating deformation even under low differential stress.

Plain Language Summary Uruguay is generally considered tectonically stable. However, here we report new evidence for tectonic activity in the area, identified by the presence of faults. These faults indicate that northwest Uruguay has experienced (or is still experiencing) tectonic deformation, with the development of minor normal and strike-slip faults. The identification of these structures is only possible through the use of high-resolution topographic data, highlighting the importance of modern data sets in assessing tectonic stability. The location and orientation of mapped faults suggest that older, inherited tectonic structures play a key role in controlling recent deformation in the area. This suggests that inherited tectonic structures act as zones of weakness that facilitate deformation over geological time scales.

Key Points:

- Topographic and field data uncovers evidence for recent tectonic activity in Uruguay
- Deformational features include fault scarp and offset streams, compatible with normal and strike-slip deformation
- Recent deformation matches location and orientation of ancient (Proterozoic and Mesozoic) inherited structures

Supporting Information:

Supporting Information may be found in the online version of this article.

Correspondence to:

M. B. Haag,
mauricio.haag@mail.utoronto.ca

Citation:

Haag, M. B., Schoenbohm, L. M., Dalla Lana Michel, R., dos Santos Scherer, C. M., Veroslavsky, G., & Marmisolle, J. (2025). Morphometric evidence for Cenozoic intraplate reactivation in NW Uruguay. *Tectonics*, *44*, e2025TC009070. https://doi.org/10.1029/2025TC009070

Received 28 JUN 2025
Accepted 6 OCT 2025

Author Contributions:

Conceptualization: Mauricio B. Haag, Lindsay M. Schoenbohm
Data curation: Mauricio B. Haag, Rossano Dalla Lana Michel, Josefina Marmisolle
Formal analysis: Mauricio B. Haag
Funding acquisition: Lindsay M. Schoenbohm, Claiton M. dos Santos Scherer
Investigation: Mauricio B. Haag, Rossano Dalla Lana Michel, Claiton M. dos Santos Scherer
Methodology: Mauricio B. Haag, Rossano Dalla Lana Michel
Project administration: Lindsay M. Schoenbohm

1. Introduction

Traditionally viewed as tectonically quiescent, intraplate landscapes are increasingly recognized as sites of subtle but geologically significant deformation (Muir et al., 2023; Salomon, Koehn & Passchier, 2015, Salomon, Koehn, Passchier, Hackspacher & Glasmacher, 2015). In many passive margins and cratonic settings, an increasing number of studies show that ancient zones of weakness, such as shear zones, can influence tectonics, present-day topography, and drainage architecture, long after the cessation of major tectonic activity (Fontainha et al., 2021; Heron et al., 2016; Salomon, Koehn & Passchier, 2015, Salomon, Koehn, Passchier, Hackspacher & Glasmacher, 2015). These inherited structures can be reactivated under far-field stress regimes, producing deformation patterns that are easily overlooked or hard to recognize in low-relief terrains (e.g., Giona Bucci & Schoenbohm, 2022).

Located in South America, the Basaltic Plateau in northwestern Uruguay is a vast (~35 thousand km^2) low-relief region characterized by local topography less than <35 m/km (Kröhling et al., 2014). This landscape is underlain by an extensive sequence of Cretaceous basalts, partially overlying sedimentary rocks of the Paraná basin, both emplaced atop a complex Precambrian basement that includes several major Proterozoic shear zones (Oriolo et al., 2018; Passarelli et al., 2011). Although typically classified as tectonically stable, historical seismicity and

Resources: Lindsay M. Schoenbohm, Claiton M. dos Santos Scherer, Gerardo Veroslavsky
Supervision: Lindsay M. Schoenbohm
Validation: Mauricio B. Haag, Lindsay M. Schoenbohm, Claiton M. dos Santos Scherer, Gerardo Veroslavsky, Josefina Marmisolle
Visualization: Mauricio B. Haag
Writing – original draft: Mauricio B. Haag
Writing – review & editing: Mauricio B. Haag, Lindsay M. Schoenbohm, Rossano Dalla Lana Michel, Claiton M. dos Santos Scherer, Gerardo Veroslavsky, Josefina Marmisolle

recent geophysical studies suggest that Uruguay remains sensitive to changes in the far-field stress regime imposed by the Andean orogeny (Baxter & Smith, 2020). Furthermore, the Basaltic Plateau features extensive topographic lineaments (Blanco et al., 2021; Marmisolle et al., 2016) and fluvial network anomalies commonly associated with structural control and recent tectonic activity (Sánchez Bettucci et al., 2025). Despite these observations, the relationship between topography, drainage network geometry, underlying structural inheritance, and potential tectonic reactivation in this region remains poorly understood.

In this study, we combine high-resolution topographic analysis with field-based structural observations to investigate whether the reactivation of ancient shear zones controls the geomorphic evolution of the Basaltic Plateau in NW Uruguay. Our findings suggest recent deformation in this region, with strike-slip deformation along pre-existing NW-SE and ENE-WSW-striking structures. Structural lineaments exert strong control over drainage pattern and orientation, and control the occurrence of minor (up to 10 m) fault scarps, offset channels, and incised valleys. These patterns suggest ongoing reorganization of fluvial systems as a result of this deformation, and therefore indicate some degree of tectonic activity. Our findings contribute to a growing body of evidence suggesting that intraplate regions are subject to subtle tectonic signals in settings otherwise considered tectonically dead.

2. Geologic Setting

We focus on a low-relief surface known as the Basaltic Plateau located in NW Uruguay (Figure 1a) (Kröhling et al., 2014). The Basaltic Plateau features extremely low relief (typically less than 35 m/km) and maximum surface elevation of up to 350 m asl (Figure 1b). Located more than 500 km away from the Atlantic coast, this area has been considered largely tectonically inactive since the opening of the South Atlantic Ocean at ca. 120 Ma (Panario et al., 2014). To the east, the Basaltic Plateau is bounded by a regional escarpment along the Negro River watershed, while to the west the Plateau gently grades to the Uruguay River (Figure 1a), with an average regional slope of <1°.

The Basaltic Plateau is mainly composed of volcanic rocks of the Paraná-Etendeka Large Igneous Province (Lower Cretaceous) emplaced in the Norte Basin (de Santa Ana, 1989), locally grouped into the Arapey Formation (de Santa Ana and Veroslavsky, 2003; Preciozzi et al., 1985). The volcanics overlie sedimentary siliciclastic rocks of the Paraná Basin (de Santa Ana and Veroslavsky, 2003; Scherer et al., 2023), including fluvial-eolian and marine deposits (Amarante et al., 2019; Manna et al., 2025; Scherer et al., 2023). Recently, geochemical studies revealed the presence of Cenozoic (51–64 Ma) alkaline volcanic vents in the Basaltic Plateau (Muzio et al., 2022). These units both overlie the Nico Pérez and Piedra Alta basement terranes (Archean-Proterozoic; Oriolo et al., 2016), which were extensively deformed during Gondwana Amalgamation during the Proterozoic (Preciozzi et al., 1985). These orogenies involved the accretion of several tectonic terrains and the development of notable, crustal-scale shear zones, mainly oriented along NE-SW to NNE-SSW (Oriolo et al., 2018; Passarelli et al., 2011).

Previous studies have mapped important lineaments traversing the Basaltic Plateau (Marmisolle et al., 2016; Morales et al., 2021; Rodríguez, Marmisolle, et al., 2015, Rodríguez, Veroslavsky, et al., 2015; Veroslavsky et al., 2019, 2021, 2024). Although no dedicated neotectonic investigations have yet been carried out, subsurface mapping based on seismic, magnetotelluric, gravimetry and borehole interpretations (e.g., Marmisolle et al., 2016; Morales et al., 2021; Rodríguez, Marmisolle, et al., 2015, Rodríguez, Veroslavsky, et al., 2015; Veroslavsky et al., 2019, 2021, 2024), reveal NW-SE and ENE-WSW-striking faults that have been shown to control both the deposition and deformation of the basement and overlying Mesozoic sequences (Figures 1c, 2a, and 2d; Marmisolle et al., 2016; Veroslavsky et al., 2019, 2021). For example, Veroslavsky et al. (2021) combined borehole and surface geological data to document normal displacements affecting the Cretaceous Arapey Formation. Relevant to the Cenozoic evolution of NW Uruguay, Blanco et al. (2021) demonstrated that NW–SE striking lineaments reflect normal faulting, which controlled the development of depocenters that accommodated Cenozoic depositional sequences (e.g., the Fray Bentos and Salto Fm). Among these structures, the Lunarejo, Arroyo Las Cañas, and Arapey/Sarandí del Yí Lineaments are the most prominent features in the study area (Figure 2b). Notably, these structures are clearly identifiable in gravimetric maps (Figure 2a).

Recent seismicity in Uruguay is concentrated in the Río de la Plata estuary (Baxter et al., 2021), although notable onshore earthquakes are documented (Sánchez Bettucci et al., 2025), mostly along the Sarandí del Yí Lineaments (Figure 1a). The 1948 events (M_L 5.8 and 5, and moment magnitude M_W, 5.8) are among the most significant

10.1029/2025TC009070

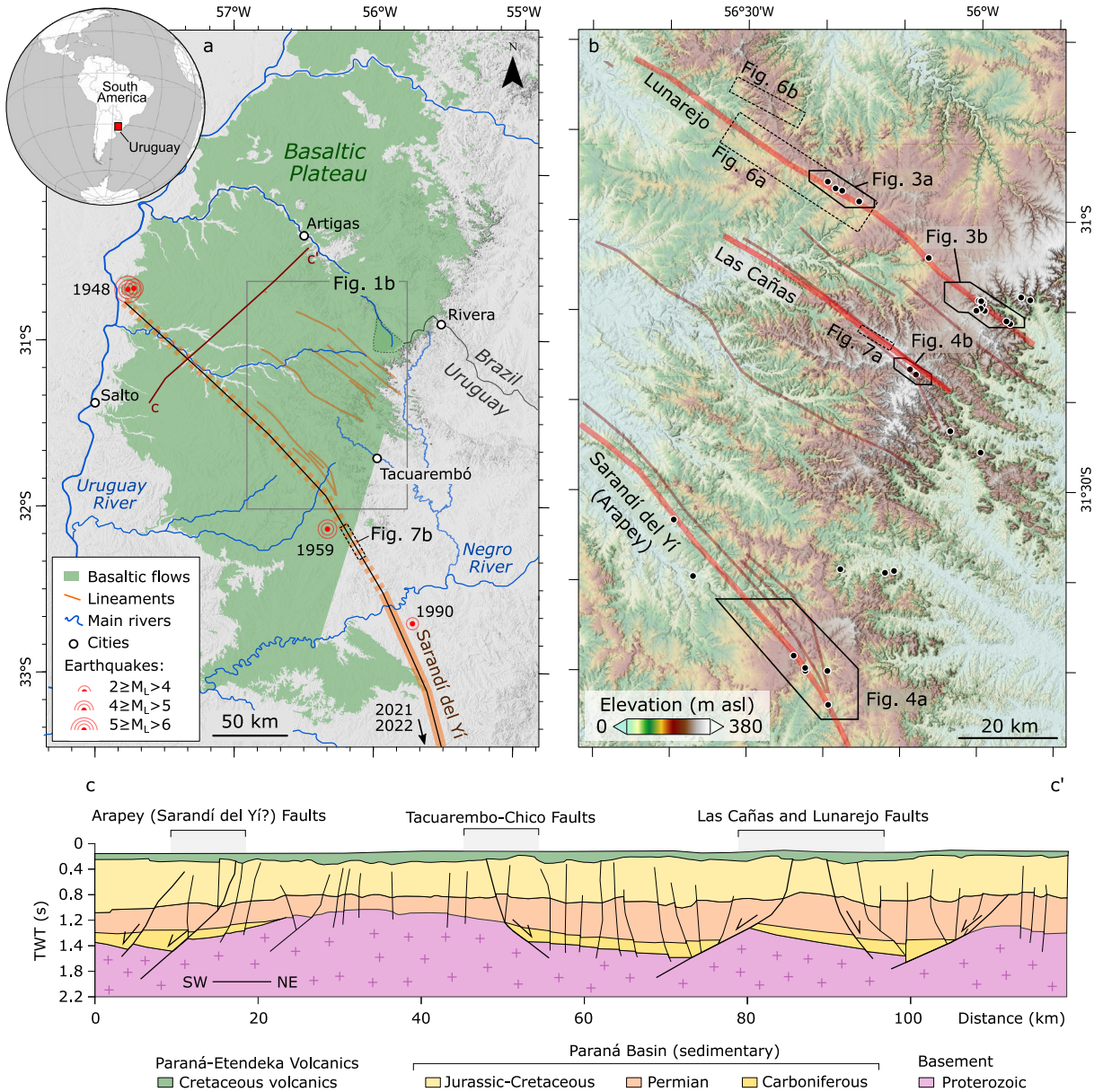

Figure 1. Study setting. (a) The basaltic plateau in NW Uruguay, with onshore earthquakes with local magnitude (M_L) ≥2 (Sánchez Bettucci et al., 2025). (b) Elevation map of the study setting, highlighting visited sites (black dots) and interpreted topographic lineaments. (c) NE-SW interpreted seismic section highlighting the presence of inherited structures in the Basaltic Plateau (adapted from Veroslavsky et al., 2021); TWT denotes two-way traveltime. Additional cross sections are provided in Figure S1 in Supporting Information S1.

events documented in onshore Uruguay (Baxter et al., 2021; Sánchez Bettucci et al., 2025), followed by the 1959 (M_L 5.0) earthquake and more recent moderate events including the 1990 (M_L 3.0) and the 2021 and 2022 (M_L 3.7 and 3.9, M_W 4.3) events (Figure 1a; Baxter et al., 2021; Sánchez Bettucci et al., 2025).

3. Methods

3.1. Inherited Structure, Lineament and Fluvial Network Analysis

We use topographic data to investigate reactivation and recent tectonic activity in the Basaltic Plateau, including identifying topographic lineaments, drainage anomalies, and potential fault escarps (e.g., Li et al., 2022). To this end, we make use of two digital elevation models (DEMs): the 12.5 m/pixel ALOS-PALSAR from the ASF DAAC (JAXA, 2014) and the 2.5 m/pixel IDEuy from the Infraestructura de Datos Espaciales de Uruguay

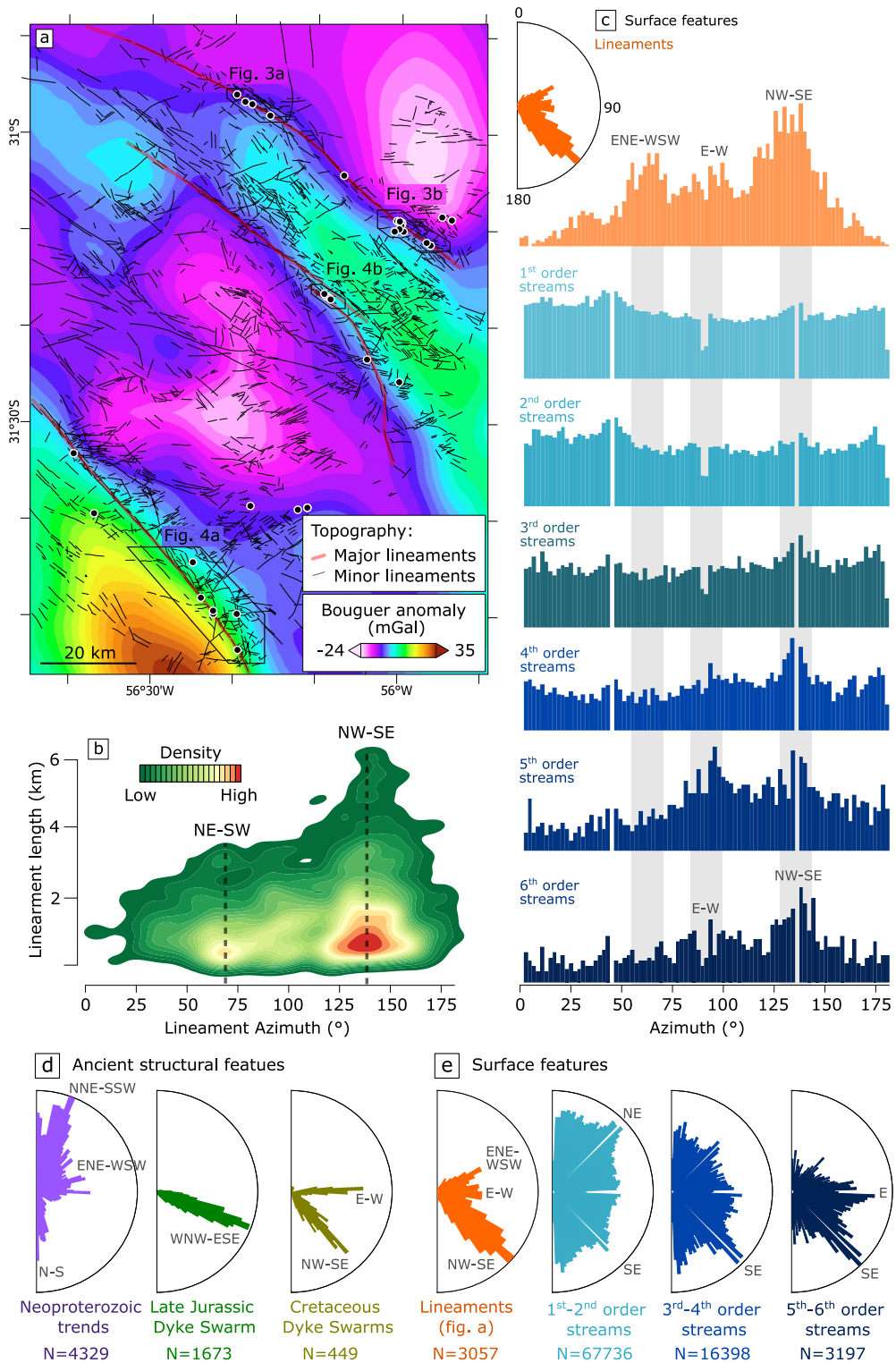

Figure 2. Lineament orientation and length. (a) Lineament distribution map underlain by Bouguer anomaly map (Rodríguez, Veroslavsky, et al., 2015). (b) Density diagram of lineament orientation versus length. (c) Lineament and river orientation histograms. ENE-WSW, E-W, and NW-SE orientations are highlighted. Rose diagrams of (d) ancient structural trends mapped in the Uruguayan shield (Núñez Demarco et al., 2020) and (e) present-day surface features. *N* indicates the number of measured structures.

(IDEuy, 2018). We conduct detailed topographic analyses along lineaments that exhibit evidence of vertical displacement, which may be used to estimate fault throw (Figures 6 and 7). For this analysis, we applied the method of Avouac (1993), which estimates throw by extrapolating elevation profiles across both sides of a potential fault trace. While this approach can provide reliable throw estimates, it does not yield information on the number of events that produced the observed offset or on the timing of these events.

Fault damage can facilitate erosion and therefore exert a control on fluvial network orientation, resulting in surface features that reflect structural features (e.g., Kirkpatrick et al., 2020). We use the 2.5 m/pixel IDEuy DEM to derive hillshade and slope maps for the study area. Hillshade maps are used to manually identify topographic lineaments using different illumination orientations (azimuths 045, 135, 225, and 315) at a 1:10,000 scale within the Basaltic Plateau. Combined with slope data, hillshade maps are also used to identify major, regional lineaments (Figure 1a) and potential fault scarps.

Planform analysis of drainage networks provides valuable insights into lithological and tectonic controls on landscape evolution (Pereira-Claren et al., 2019). To examine drainage patterns and stream orientation, we use TopoToolbox 2.3 (Schwanghart & Scherler, 2014) to extract the drainage network from the high-resolution IDEuy DEM. Then, we examine the drainage network for drainage anomalies (e.g., offset channels, barbed tributaries, deflected channels, faceted spurs, and incised valleys). To assess the influence of topographic lineaments on drainage patterns, we analyzed stream orientations using 100 m-long river segments located within a 2-km buffer zone around each lineament (Figure S2 in Supporting Information S1). This analysis was conducted separately for different stream orders following the Strahler classification. River directions along the 0, 45, 90, and 135 ± 1° azimuths were excluded due to artifacts introduced by the flow routing algorithm (Schwanghart & Scherler, 2014) (see Figure S2 in Supporting Information S1).

We identified the presence of underlying inherited structures through a synthesis of existing geophysical and geological data sets for Uruguay, including seismic profiles, borehole data, gravimetry, and magnetometry. Gravimetric data from Rodríguez, Veroslavsky, et al. (2015) were used to delineate major structural lineaments across the study area (Figure 2a). Although high-resolution magnetometry data are unavailable for the basaltic plateau itself, we incorporated data from the Uruguayan Shield located further south (Núñez Demarco et al., 2020). Despite not being directly beneath the study area, the Uruguayan Shield belongs to the same structural province, therefore featuring similar tectonic fabrics. Therefore, it is reasonable to expect that these regional lineaments extend northward into the Basaltic Plateau. Using data sets compiled by Núñez Demarco et al. (2020), we extracted the orientations of Proterozoic and Mesozoic structural trends and major dike swarms within the Uruguayan Shield (Figure 2d). These orientations provide a framework for interpreting structural inheritance in the overlying basaltic units. Additionally, borehole records and seismic sections from the basaltic plateau (e.g., Marmisolle et al., 2016; Veroslavsky et al., 2019, 2021, 2024) offer direct subsurface evidence for structural lineaments (Figure 1a).

3.2. Field Observations and Structural Data Collection

Outcrop scale fracture networks can be used to track zones of increased deformation and gain insight into larger tectonic processes (Panara et al., 2024; Tibaldi et al., 2021). On the basis of our observations of topographic and drainage anomalies, we identified four field areas for additional study and validation (Figures 3 and 4, location in Figure 1b). We examined these sites using a combination of outcrop and aerial photograph mapping of river channels and bedrock exposures. Note that despite the thin soil cover, the region is generally covered and of low relief, meaning that quality exposures are limited.

We collected aerial imagery with a UAV model DJI Mavic 2 Pro, which allowed us to obtain detailed images (Figures 8 and 9) with a spatial resolution of ∼1 mm/pixel. Using Agisoft Metashape, we generate an orthomosaic for each area and perform detailed lineament mapping on these outcrops. For each field area, we map fracture patterns, including orientations, length, and spacing (e.g., Peace & Jess, 2023). This analysis enables us to compare outcrop-scale fracture patterns with regional-scale structural lineaments.

To determine deformation patterns in the study area, we performed structural field measurements at 23 sites across these four field areas, where we were able to identify good exposures of fractured bedrock (Figures 3 and 4). We measured the orientations of fractures using an iPad Mini 2 and the software Clino following the recommendations of Pascal (2022). We use Stereonet 11 (Cardozo & Allmendinger, 2013) to process field data,

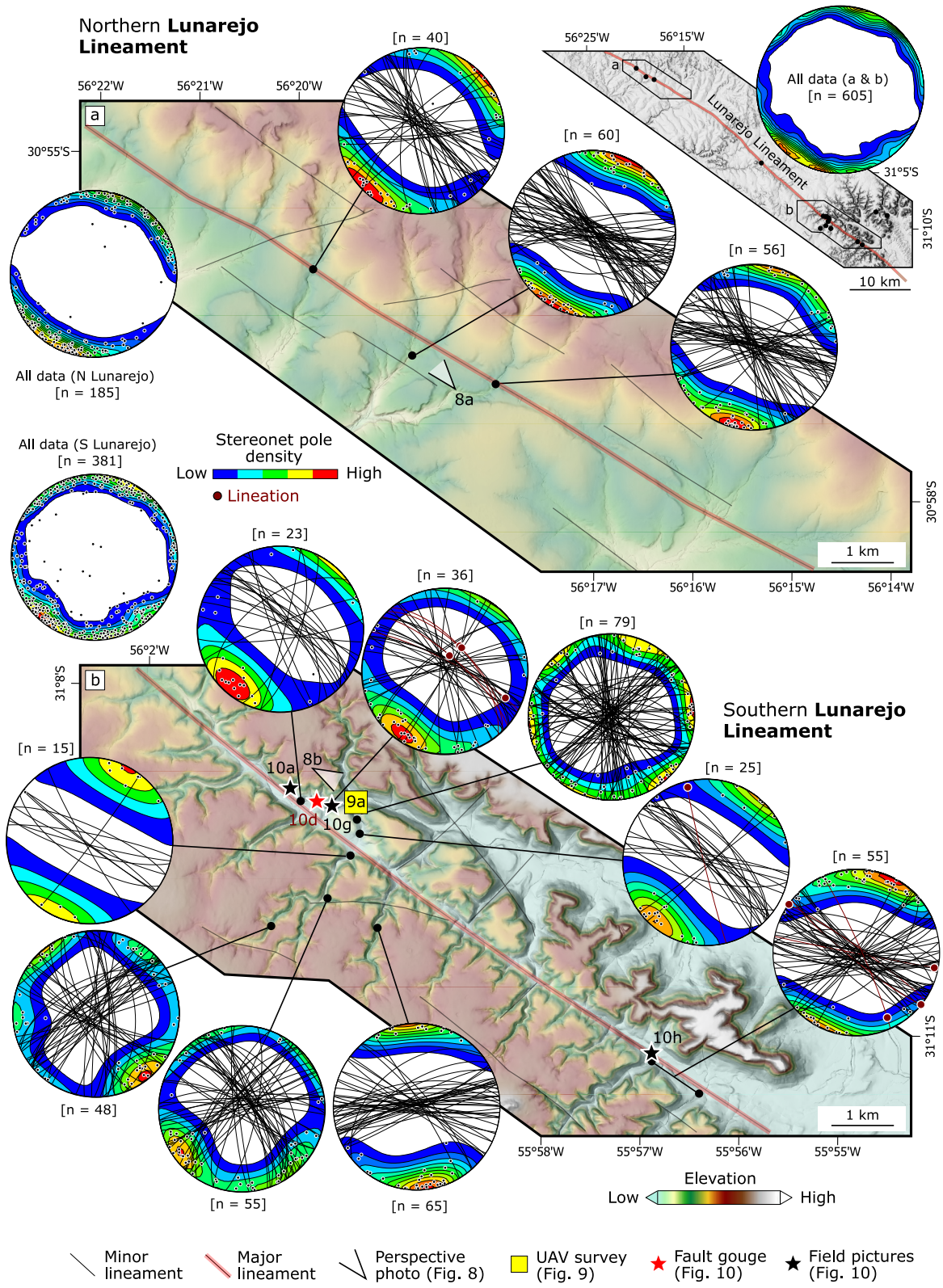

Figure 3. Lunarejo Lineament. (a) northern section of the Lunarejo Lineament, with three measured sites. (b) southern section of the Lunarejo Lineament, with a total of nine sites. Locations shown in Figures 1b and 2a.

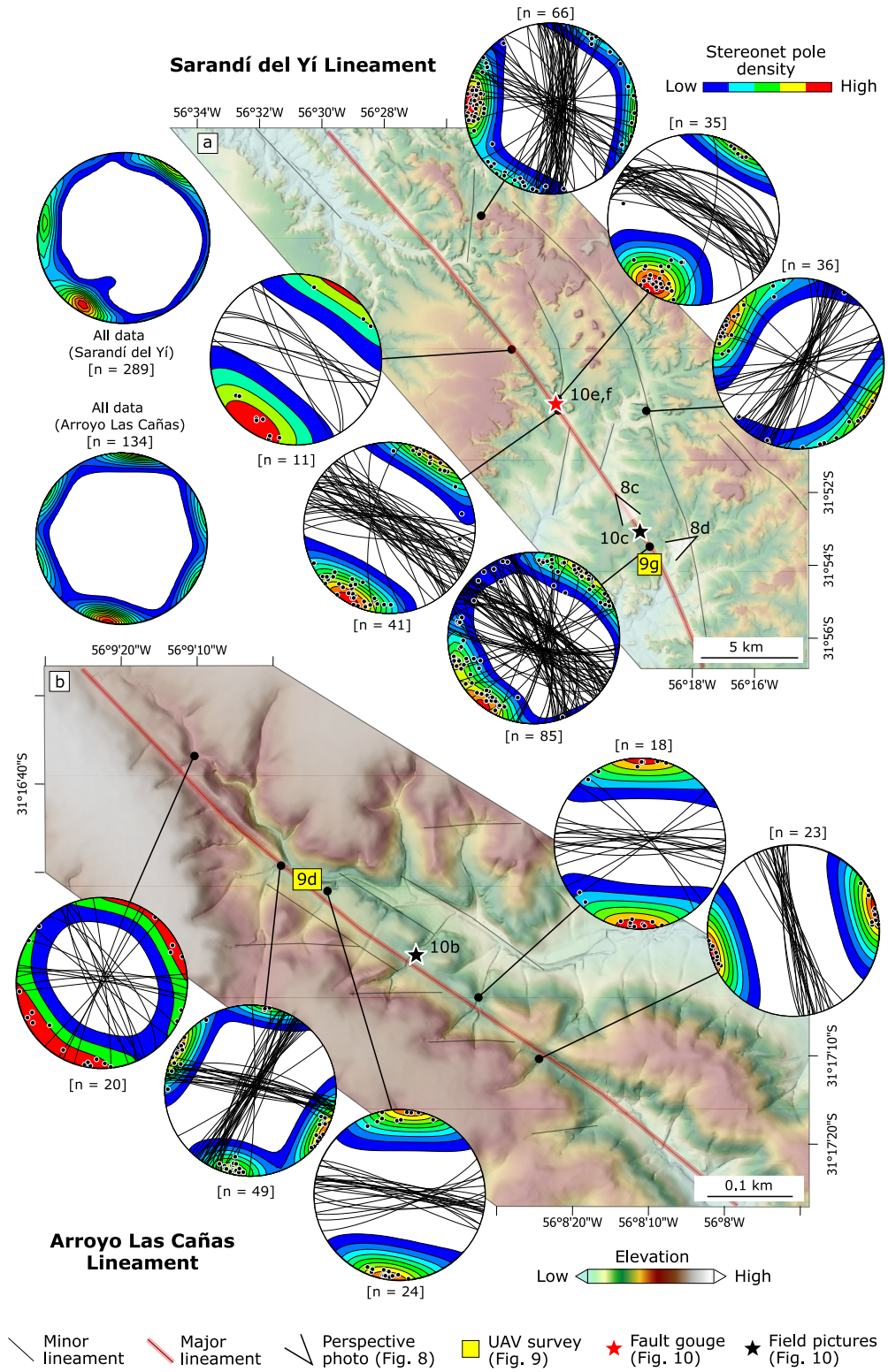

Figure 4. (a) Sarandí del Yí Lineament, with seven measured sites. (b) Arroyo Las Cañas Lineaments, with a total of five sites. Locations shown in Figures 1b and 2a.

which were grouped using stereonets, rose diagrams, and/or density plots. Due to the scarcity of kinematic indicators (e.g., striations) in the examined outcrops, conducting a paleostress inversion was not feasible in the study area.

4. Results

4.1. Lineament and Stream Orientation

Based on high-resolution DEMs, we mapped over 3,000 topographic lineaments in the study area (Figure 2a). We identify and predominance of NW-SE striking (~135° azimuth) lineaments in the region (Figure 2a), which show higher frequency and longer length than lineaments with other orientations (Figure 2b). This prominent NW-SE orientation is also seen in the orientation of segments of the stream network at all orders (Figure 2c). There is a secondary trend of lineaments with an approximately ENE-WSW orientation (~70° azimuth; Figures 2b and 2c). Interestingly, the stream network does not reflect this trend but rather shows alignment orthogonal to the main lineament direction (NE-SW). A tertiary trend of stream segments-oriented E-W (~90° azimuth) is most apparent only for higher order (>3rd) streams (Figure 2c).

The major surface lineaments we mapped using DEMs closely align with the orientations of subsurface structures inferred from gravimetric data (Núñez Demarco et al., 2020; Figure 2a). Ancient structural trends, spanning from the Proterozoic to the Mesozoic, show a predominance of N–S, NNE–SSW, and E–W orientations within Archean-Proterozoic basement (Figure 2d; Núñez Demarco et al., 2020). In contrast, Mesozoic dike swarms exhibit WNW–ESE, NW–SE, and E–W trends. NW-SE and E-W-striking structures are closely aligned with regional surface lineaments, as well as major river orientations (Figure 2e).

The NW-SE trend in lineament orientation is apparent at a smaller scale of observation across the Basaltic Plateau as well, particularly along northern and southern Lunarejo (Figures 3a and 3b), Arroyo Las Cañas (Figure 4b), and Sarandí del Yí (Figure 4a) lineaments. E-W to ENE-WSW lineaments are particularly common in the Lunarejo region, where these structures appear to control the development of river valleys (Figure S3 in Supporting Information S1). Locally, lineaments appear to influence and disrupt drainage patterns, as evidenced by the rectangular planform of fluvial network observed in these regions (Figure 5).

4.2. Drainage Reorganization and Topographic Evidence for Deformation

Inspection of drainage patterns and topography along major lineaments reveals the presence of potential fault scarps, offset channels, and drainage divides that are consistent with fluvial network reorganization near topographic lineaments (Figure 5) (e.g., Duvall & Tucker, 2015). For example, just north of the Lunarejo Lineament, offset channels are compatible with either down-to-the-NE displacement along a dip-slip fault or with right-lateral strike-slip displacement (Figures 5a and 5b). This region also features growing channels with decreasing drainage toward the leading edge of lineament (Figure 5b; Duvall & Tucker, 2015), compatible with right-lateral displacement. Along the Lunarejo Lineament, a potential fault scarp separates incised from non-incised fluvial valleys, indicating dip-slip faulting (Figures 5c and 5d). Further south along the same lineament, the Lunarejo Valley features offset channels compatible with left-lateral displacement (Figures 5e–5g). Although interpretation of strike-slip disruption of drainage networks is complicated, the upstream nature of displacement in some of these examples (Figure 5f) supports this interpretation. Similarly, scarps are also present along the Arroyo Las Cañas Lineament, with minor vertical displacements (Figures 5h and 5i). In the Sarandí del Yí Lineament, a wide (~50 m) valley is developed parallel to the lineament strike, denoting enhanced erosion along NW-SE lineaments (Figures 5j and 5k).

Detailed topographic profiles from lineaments reveal minor vertical displacements, compatible with throw measurements of 2.9–5.1 m in the northern Lunarejo segment (Figure 6a). In the middle part of the Lunarejo lineament, where vertical displacements are observed on opposite sides of the lineament (Figure 5a), estimated throw measurements are highly variable, ranging from 6.3–11.2 m (Figure 6b). The apparent reversal of throw along strike likely reflects strike-slip displacement and horizontal offset of topographic features, possibly in a right-lateral sense, rather than a change in dip-slip displacement. Further south in the study area, the Las Cañas lineaments features throw estimates of 6.9–12 m, including displacements along a subsidiary structure (Figure 7a). Similarly to along the Lunarejo lineament (Figure 6b), throw estimate along the Sarandí del Yí Lineament are highly variable and occur on opposite sides of the lineament, possibly also indicating right-lateral

10.1029/2025TC009070

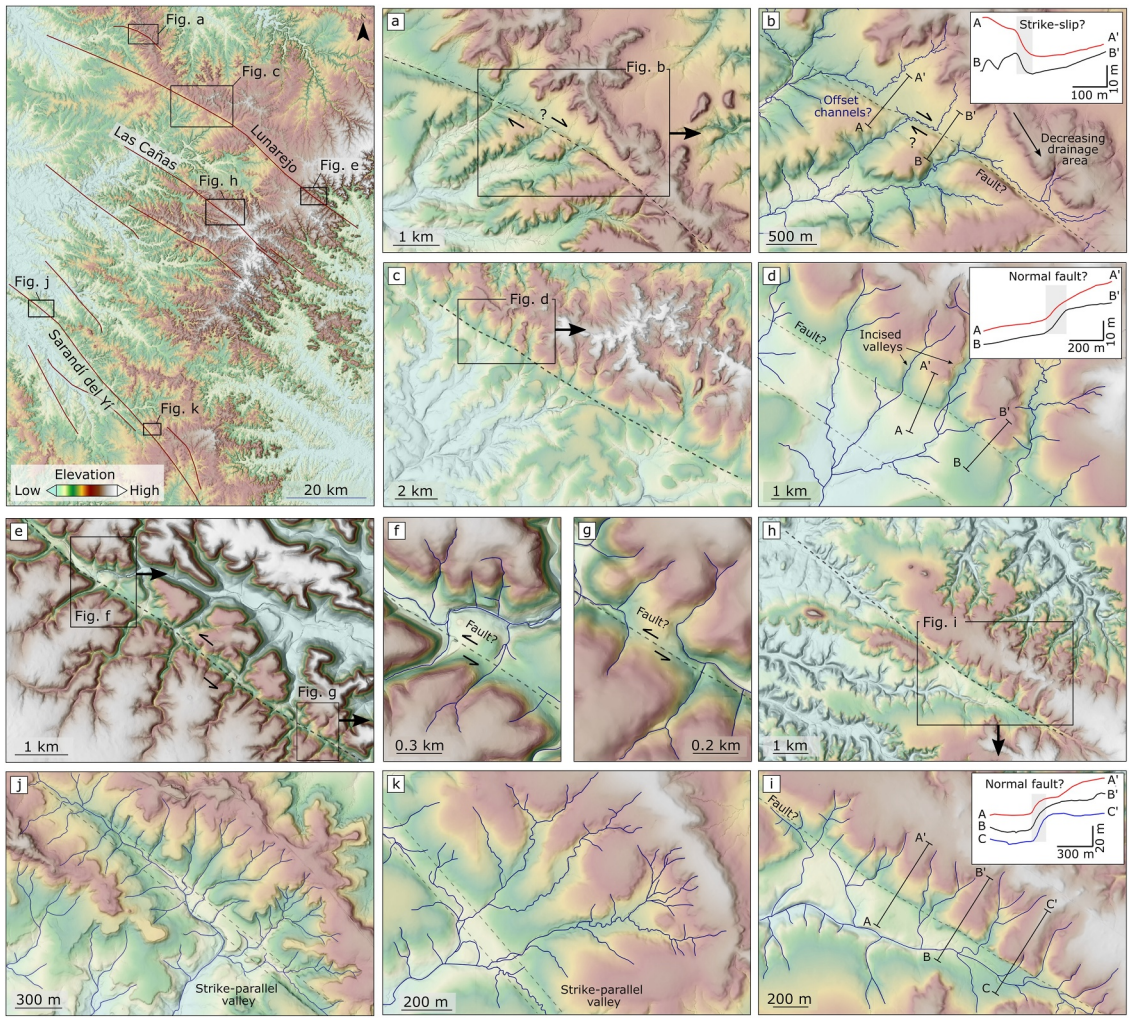

Figure 5. Potential evidence for drainage reorganization as response to tectonics in the Basaltic Plateau. (a–b) Offset channels and faut scarp in subsidiary structure near the northern Lunarejo Lineament; (c–d) Fault scarps and differential incision in the northern Lunarejo Lineament; (e–g) Potential offset channels along the southern Lunarejo Lineament; (h–i) Fault scarps and differential incision in the northern Las Cañas Lineament. (j–k) concentrated/preferential incision along NW-SE-striking river valleys. Locations of (a–j) are shown in the upper left inset.

displacement along a strike-slip fault (Figure 7b). Slope measurements along topographic profiles are reported in Figures S4 and S5 in Supporting Information S1.

4.3. Field Observations

The Basaltic Plateau is characterized by extensive flat to gently sloping surfaces, with minimal (<5 m) fluvial incision observed near the headwaters. Soil cover is generally thin (<1 m), and sparse, small bedrock outcrops can be located across the study area (Figures 8a and 8c). In contrast, relatively deeply incised channels (~50 m) dominate the landscape of the eastern escarpment in the Lunarejo Valley region (Figure 8b). Notably, these channels are predominantly devoid of sediment (Figure S6 in Supporting Information S1).

Field inspection along major lineaments identified in DEMs (Figure 2) reveals the presence of a strong association between topographic lineaments, fractured bedrock, and river channels (Figure 8). In the Northern Lunarejo lineament (Figure 8a), a major NW-SE lineament is associated with linear depressions in the field (Figure 8a). Inspection of these features reveals thin soil underlain by extensively fractured and weathered bedrock (Figure S7 in Supporting Information S1). In the Lunarejo region (Figure 8b), NW-SE lineaments are associated with incised (~50 m), linear valleys (Figure 8b). Along the projected trace of the Sarandí del Yí shear zone (Figure 8c) we also

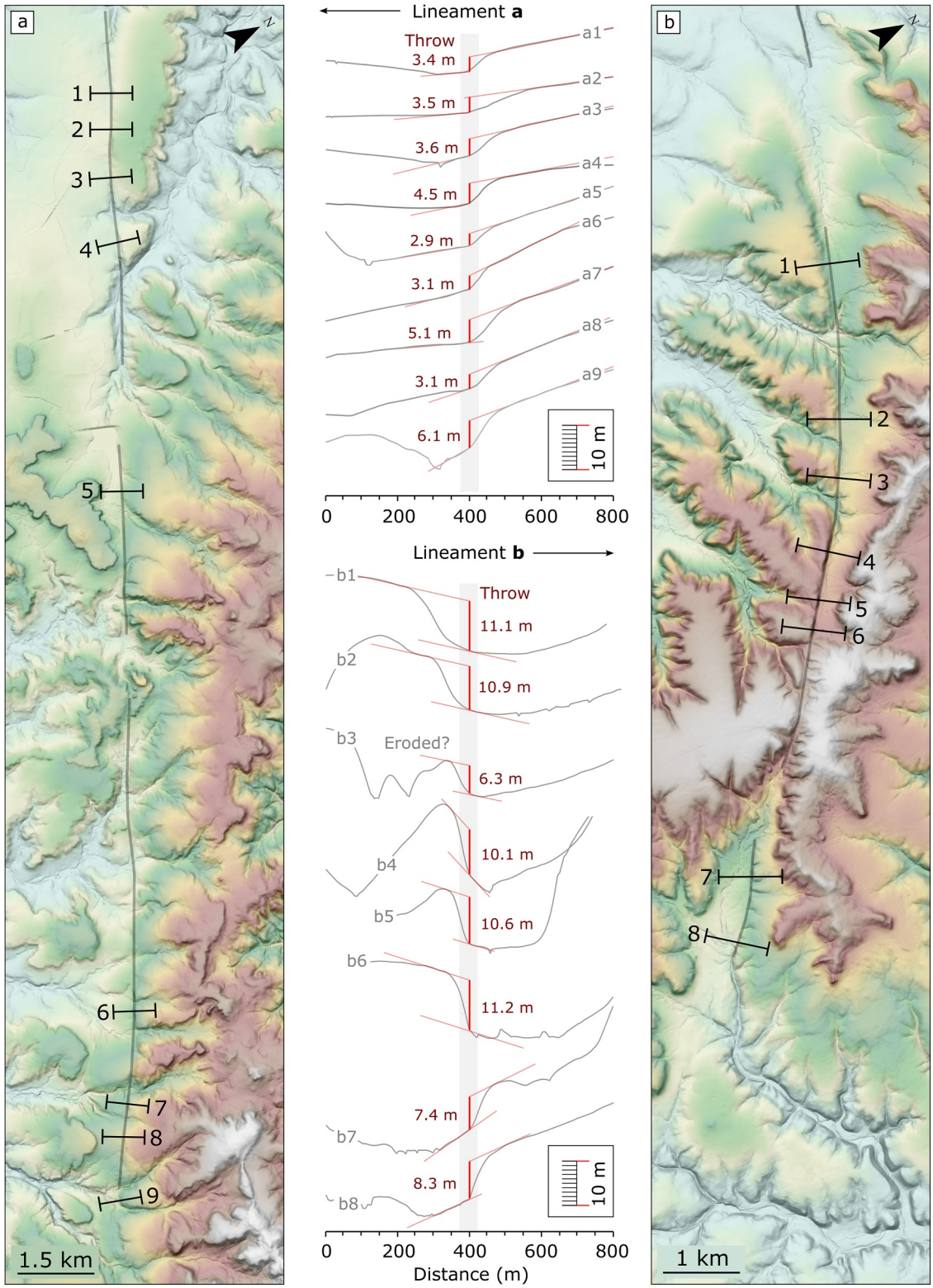

Figure 6. Topographic profile along potential fault traces in the Basaltic Plateau obtained using the high-resolution (2.5 m/pixel) digital elevation model (IDEuy, 2018). (a) Northern Lunarejo Lineament, featuring throw measurements up to ~6 m. (b) ~10 km north of the northern Lunarejo Lineament, featuring throw estimates between 6–12 m; location shown in Figure 1b.

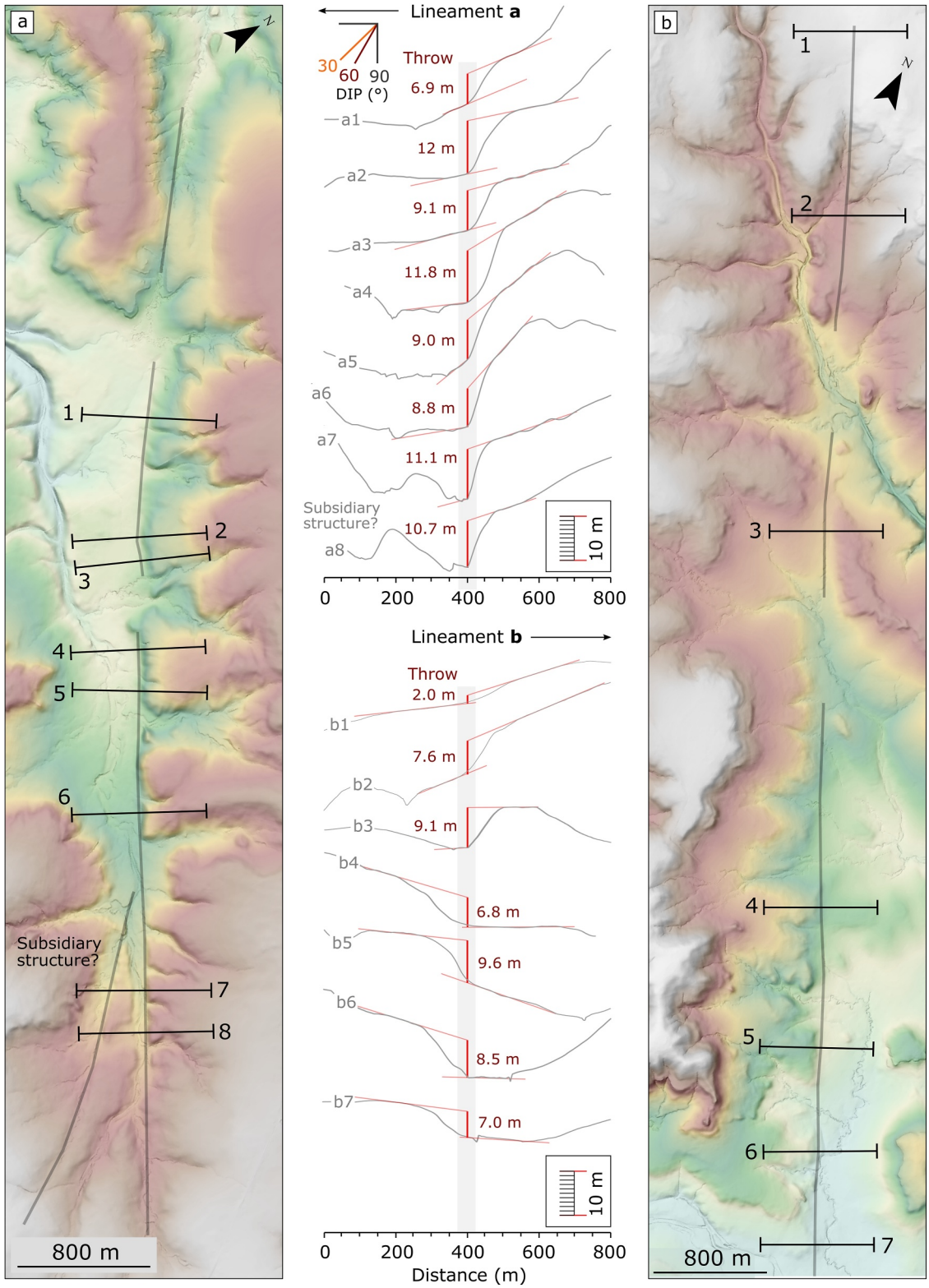

Figure 7. Topographic profile along potential fault traces in the Basaltic Plateau obtained using the high-resolution (2.5 m/pixel) digital elevation model (IDEuy, 2018). (a) Las Cañas Lineament, featuring throw measurements between 7–12 m; location shown in Figure 1b. (b) Southern segment of the Sarandí del Yí Lineament, featuring throw estimates between 2–10 m; location shown in Figure 1a.

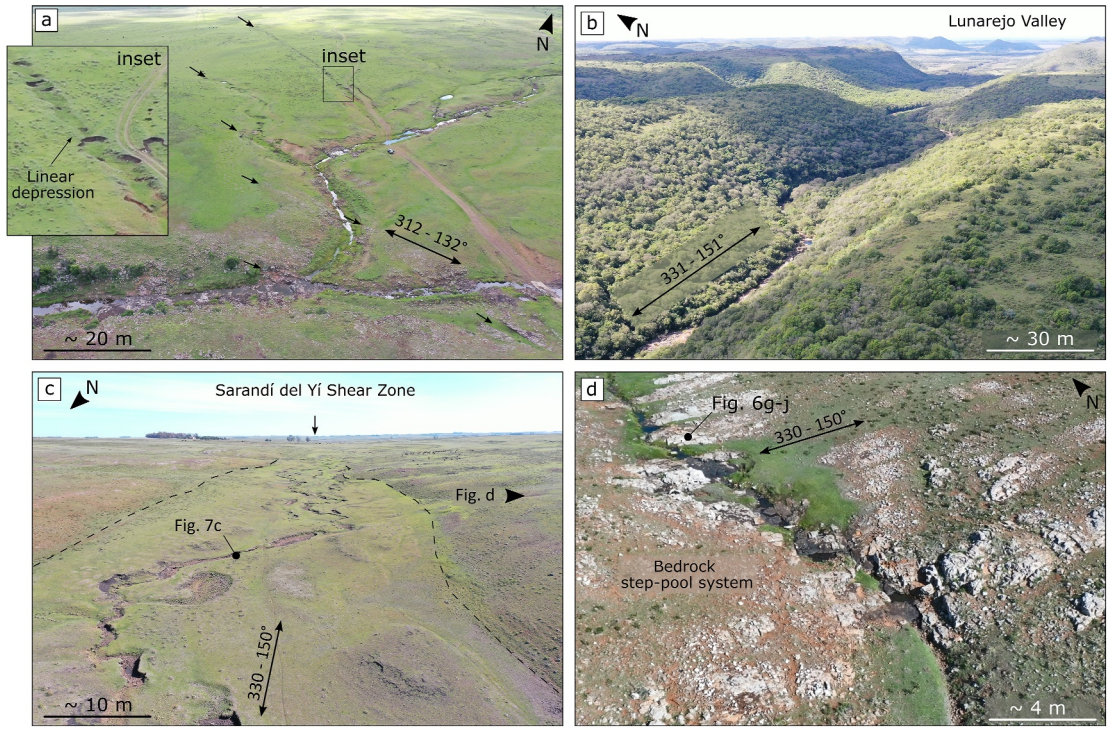

Figure 8. Field aspects of topographic lineaments. (a) Circular depressions along lineament trace in the northern Lunarejo Lineament (location in Figure 3a); (b) Incised fluvial valley in the southern Lunarejo Valley (location in Figure 3b); (c) Fluvial system overlapping the Sarandí del Yí Shear Zone (location shown in Figure 4a). (d) Extensively fractured bedrock along the channel walls, with a step-pool system (location shown in Figure 4a).

observe a linear, fluvial depression. In this region, a series of closed depressions, similar to those observed in the Northern Lunarejo lineament region, are also present, but here at larger scale (Figure 8c).

High-resolution UAV images reveal extensively fractured basaltic flows across all examined regions (Figure 9). Fractures identified at outcrop scale using UAV generally align with major structural features, with a dominance of NW-SE and ENE-WSW-striking structures, with NW-SE sets being most prevalent (Figure 9). Locally, NW-SE fracture sets control the orientation of drainage networks, as exemplified in bedrock rivers along the Lunarejo Lineament (Figure 9a). Although NW-SE sets are the most prevalent, ENE–WSW fracture sets also appear prominently in several regions (Figures 9b and 9c). Along the Las Cañas Lineament (Figure 9d), UAV imagery reveals fracture sets consistent with shear along NW–SE planes, including the development of Riedel shears indicating a right-lateral sense of shear (Figures 9e and 9f). In the southern Sarandí del Yí Lineament, NNW-SSE sets dominate, largely following the inflection of the Sarandí del Yí Lineament observed toward the south of the study area (Figure 1a).

The most common deformational features in the Basaltic Plateau are fractures (Figures 10a–10c) (sensu Pascal, 2022). Extensional (mode I) fractures are the most common structures, including joints and veins, which are typically filled with calcite and quartz. Extensional fractures are subvertical, with spacing ranging from 5–15 cm (Figures 10a–10c). In addition to fractures, basaltic breccia and fault gouge are also observed in two locations, along the Lunarejo (Figure 10d) and the Sarandí del Yí Lineament (Figures 10e and 10f). In both cases, the location of fault gouge coincides with the location of major topographic lineaments (Figures 3 and 4). Basaltic gouge and breccia are marked by the presence of alteration seams, calcite veins, and zeolite surrounding relatively unaltered basaltic clasts, ranging from mosaic to crackle breccia (Woodcock & Mort, 2008). In a few locations, a secondary set of WNW-ESE-striking fractures is also observed cross-cutting fault gouge (Figure 10e). Striations and other slip indicators are rare in the study area (Figures 10f and 10g), with occurrences primarily concentrated in the Lunarejo region. Where observed, these features indicate both dip-slip and strike-slip kinematics along NW-SE-striking structures (Figure 3b).

10.1029/2025TC009070

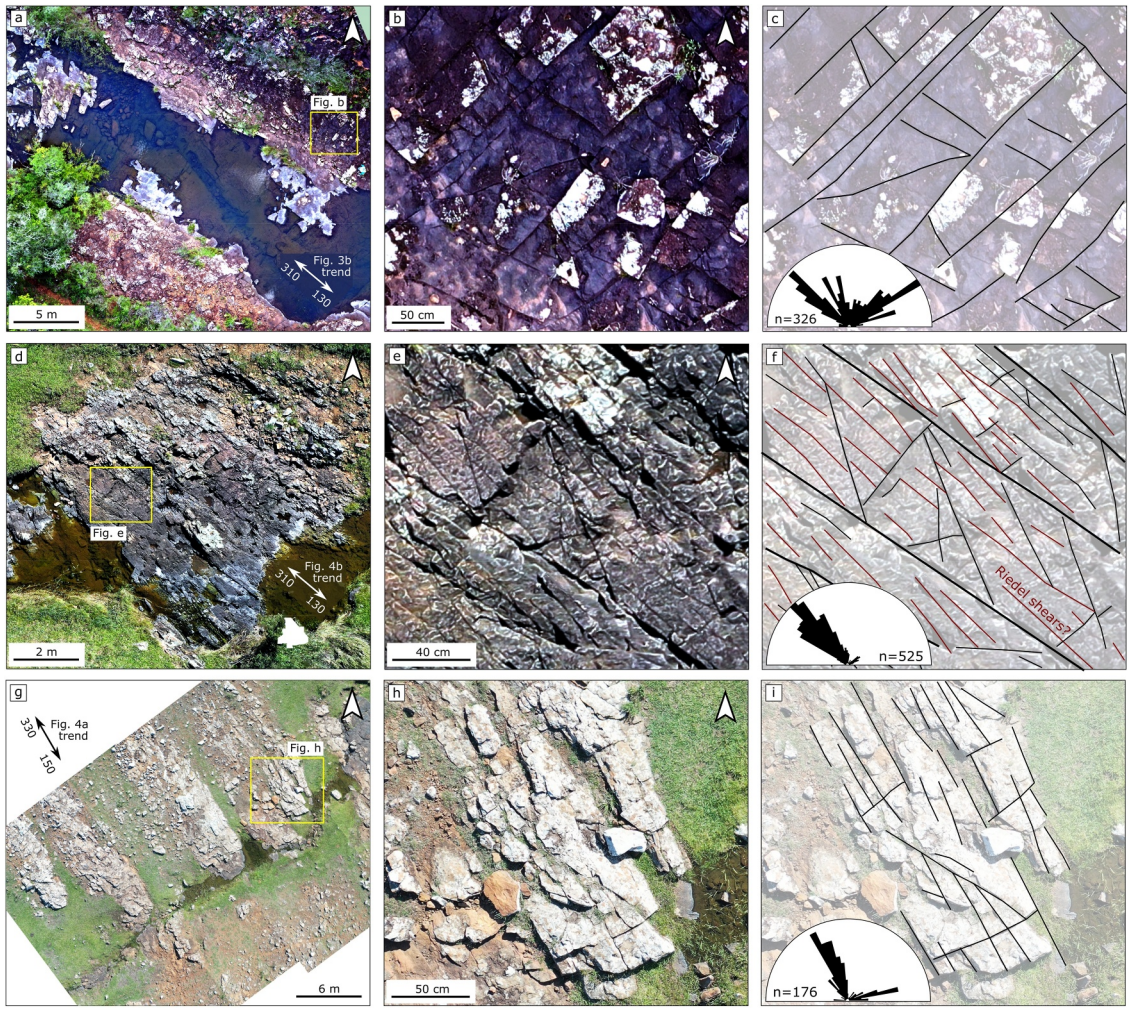

Figure 9. UAV observations and detailed fracture analysis. (a–c) Bedrock exposure along the Lunarejo Valley depicting a NW-SE fracture sets, with respective structural interpretation; location shown in Figure 3b. (d–f) Bedrock exposure along the Las Cañas region, with respective structural interpretation; location shown in Figure 4b. (g–i) Bedrock exposure in the Tacuarembó region (Sarandí del Yí lineaments) depicting a NNW-SSE fracture sets, with respective structural interpretation; location shown in Figure 4a.

5. Discussion

5.1. Evidence for Tectonic Deformation

We considered three explanations for the topographic lineaments observed in the Basaltic Plateau: dikes, preservation of ancient fault scarps, and recent tectonic deformation. Although dike swarms can form linear relief, our field observations reveal no diagnostic evidence of dikes (e.g., cross-cutting relationships, contrasting color and texture, or subvertical magmatic foliation). Instead, the mapped lineaments coincide with highly fractured zones within horizontally bedded basaltic flows (Figures 10a–10c). In addition, in adjacent regions where sedimentary rocks dominate (e.g., east of the study area, where Cretaceous strata predate the Arapey Fm. flows), there is no continuation of putative dikes from the basalt into these units. Combined, the absence of structural or lithologic evidence for intrusive rocks suggests that the mapped lineaments are unlikely to reflect dikes.

Alternatively, the mapped lineaments might represent ancient (i.e., Cretaceous) block displacements. However, over tens of millions of years, such scarps would be expected to undergo substantial degradation. Instead, the observed features form remarkably linear topographic traces with limited dissection (Figures 3 and 4). Therefore, we interpret the surface features observed in the Basaltic Plateau (Figure 5) as suggestive of Cenozoic deformation.

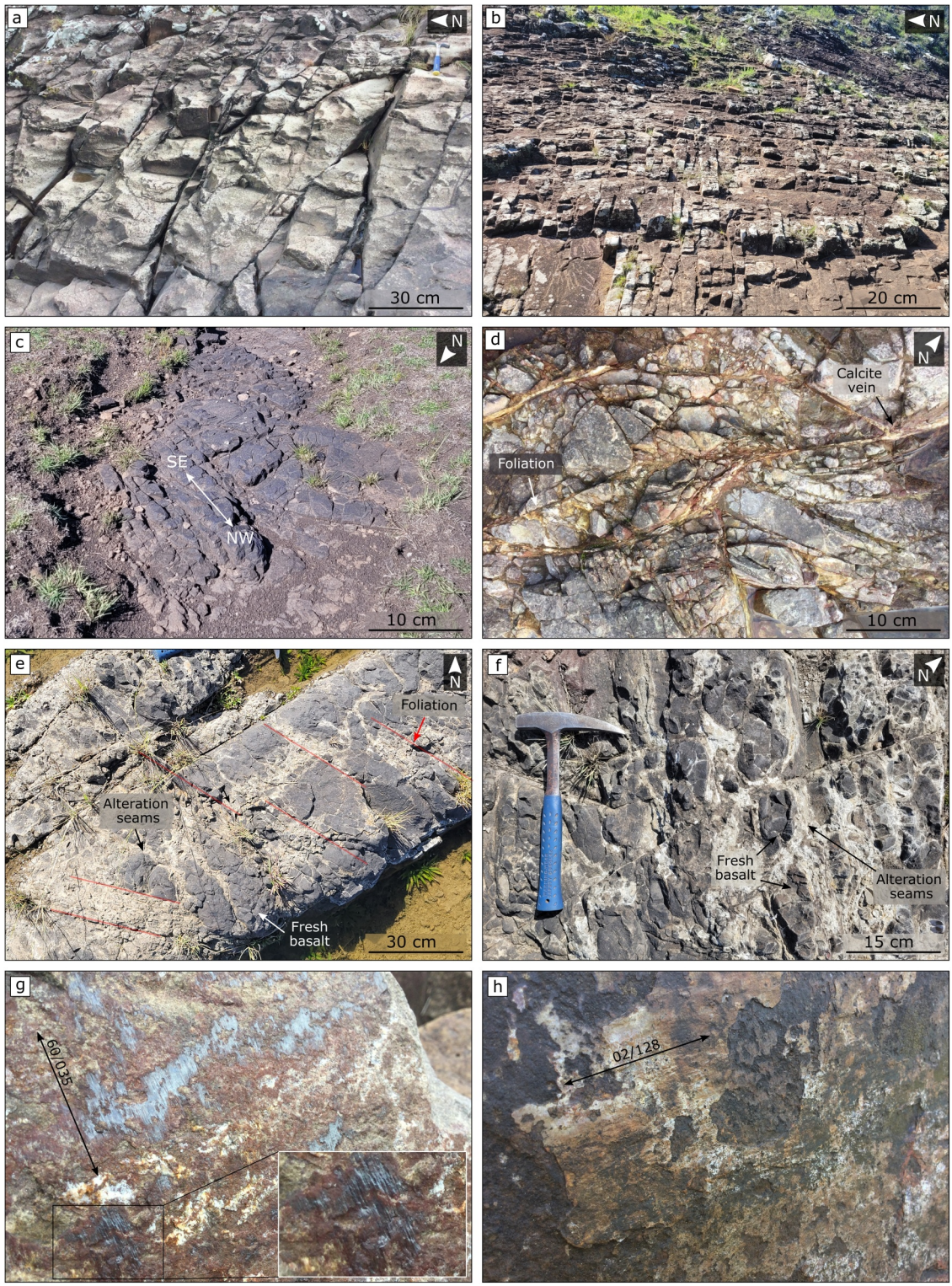

Figure 10. Deformational features in the field. (a) Irregular, nearly-vertical E-W striking structures (Figure 3a). (b) Closely-spaced vertical E-W striking structures. (c) Closely-spaced NW-SE striking fractures along the Sarandí de Yí lineament (Figure 4a). (d) Crackle basaltic breccia and fault gouge with apparent sinistral kinematics along bedrock exposure in the Lunarejo Valley (Figure 3b). (e) Mosaic basaltic breccia and fault gouge along bedrock exposure along the Sarandí de Yí lineament (Figure 4a). (f) Detailed features of fault gouge observed in (e), featuring alteration seams and fresh basaltic clasts (Figure 4a). (g) High-plunging lineations in NW-SE-striking plane. (h) Nearly horizontal lineations in NW-SE-striking plane filled with calcite.

5.2. Deformation Style

Lineament analysis reveals that post-emplacement deformation is primarily concentrated along narrow (<50 m) NW-SE-striking lineaments, and subordinate ENE-WSW-oriented structures (Figure 2). In the field, deformation is mainly developed as fractures sets (Figures 10a–10c). Although these fractures could have several origins (e.g., cooling fractures, unloading fractures, tectonic fractures; Pascal, 2022), their length, consistent orientation, and alignment with major topographic lineaments (e.g., Figures 3a, 3b, and 4a) point to a tectonic origin. Cooling fractures typically occur at the scale of individual flows and are not expected to form laterally extensive, consistently oriented structures. Although cooling fractures are common in the Basaltic Plateau (see Figure S8 in Supporting Information S1), we did not incorporate these structures into our analysis. Similarly, unloading fractures, which tend to be vertical and reflect the modern stress field or topographic unloading, would be expected to vary in orientation according to topography (Moon et al., 2017). Therefore, the consistent regional orientation and length of the lineaments are rather indicative of a tectonic origin.

This hypothesis is supported by the presence of basaltic breccias and fault gouge in two locations along the Lunarejo Lineament (Figure 10d) and in the vicinity of the Sarandí del Yi Lineament (Figures 10e and 10f). The breccias mapped in NW Uruguay resemble basaltic breccias observed in fault zones in the Faroe Islands (e.g., Walker et al., 2013; Bamberg et al., 2023, their Figure 2), Alaska (Braden & Behr, 2021), and Iceland (Karson et al., 2018), strengthening our interpretation of displacement along some of these lineaments. Although rare, the presence of lineations (Figures 10g and 10h) along major structures further supports this interpretation.

While we cannot directly constrain the dip of these structures, the predominance of extensional features in the broader region (e.g., Veroslavsky et al., 2021) suggests that normal faulting is the most likely fault mechanism. For example, the presence of vertical offsets compatible with throw measurements up to 12 m in the Lunarejo (Figures 5c, 5d, and 6a) and Arroyo Las Cañas (Figures 5h, 5i, and 7a) is broadly compatible with normal faulting (e.g., Muir et al., 2023). Additionally, the presence of offset channels located north of the Lunarejo lineament (Figures 5a and 5b), in the Lunarejo Valley (Figures 5e–5g), and in the Arroyo Las Cañas region (Figures 5h and 5i) provides geomorphic evidence for lateral (strike-slip) displacement along some lineaments in the Basaltic Plateau (Figures 6b and 7b). Inferring kinematics from geomorphic observations alone is, however, challenging. In humid landscapes like NW Uruguay, channel responses to faulting are often diffuse and variable, and a mix of large and small offsets is expected in humid regions (Reitman et al., 2019), which can obscure topographic evidence for displacement. Consequently, interpretations based solely on morphometric parameters, such as the proposed apparent switch from sinistral to dextral motion along mapped lineaments, should be treated with caution.

Therefore, the scarcity of unambiguous displacement features, combined with potentially low deformation rates, limits our ability to precisely characterize these faults and accurately quantify displacement in the Basaltic Plateau. Despite extensive field mapping, the subdued topography, homogenous lithology, low tectonic rates, and chemical weathering in the Basaltic Plateau (Garzanti et al., 2021) pose challenges to constraining fault kinematics and fully understanding the tectonic kinematics of this area.

5.3. Timing of Deformation

5.3.1. Post-Breakup (Cenozoic) Deformation

The lineaments, fractures, and fault-related features we observe in the Basalt Plateau must post-date emplacement of the Arapey basalts of ca. 133 Ma (Gomes & Vasconcelos, 2021). However, constraining the precise timing of this deformation is challenging because this region may have experienced multiple episodes of deformation, spanning from the Cretaceous to the present day.

Evidence for multiple and/or recurrent episodes of deformation throughout the Cenozoic are provided by depositional patterns northwest of the study area. In this region, NW-SE normal faults are shown to control the distribution of several Cenozoic sedimentary units (Blanco et al., 2021; Veroslavsky et al., 2019). For example, regional mapping performed by Blanco et al. (2021) reveals that the depositional pattern of the Guichón (Late Cenozoic), Fray Bentos (Oligocene), and Salto (Pliocene-Pleistocene) formations is controlled by major normal faults. Furthermore, compositional and geochemical data from these rock units suggest diagenetic processes, such as cement composition, compatible with fluid compositions that reflect fault reactivation (Blanco et al., 2021; Veroslavsky et al., 1997).

Paleostress analyses indicate that the southeastern passive margin of South America has experienced important changes in the stress field since rifting (Arioni et al., 2024; Cobbold et al., 2007; Salomon, Koehn, Passchier, Hackspacher, & Glasmacher, 2015). The presence of normal faulting documented by subsurface studies in the Basaltic Plateau (Blanco et al., 2021; Marmisolle et al., 2016, 2025; Morales et al., 2021; Veroslavsky et al., 2024) matches the E-W-directed extension identified by Santos et al. (2019) and Salamuni et al. (2021) for most of the Paleogene and Lower Miocene. Additionally, regional mapping indicates the presence of both NW–SE and ENE–WSW-striking normal faults (e.g., Blanco et al., 2021; Marmisolle et al., 2016, 2025; Veroslavsky et al., 2024; Figure 1c), suggesting shifts in the horizontal extension.

Although the precise timing of this extensional regime in northwestern Uruguay remains uncertain, horizontal neutral to extensional conditions in the Andes during the Late Paleocene–Early Eocene (Horton, 2018) could have possibly influenced the regional stress field in Uruguay (e.g., Baxter & Smith, 2020). In the Basaltic Plateau, Cenozoic horizontal extensional tectonics may be further supported by the presence of 51–64 Ma alkaline volcanic vents (Muzio et al., 2022), a period that coincides with the timing of recently proposed extension in the Andes (Bertin et al., 2025). Based on these findings, we argue that NW Uruguay has been subject to ongoing/intermittent intraplate deformation during most of the Cenozoic, including modern times (e.g., Arioni et al., 2024).

5.3.2. Recent (Quaternary) Deformation

Geodetic observations and earthquake records document notable recent seismicity across the Basaltic Plateau. For example, recent seismic activity in the Basaltic Plateau has included $M_L > 5$ events in 1948 and 1959 (Sánchez Bettucci et al., 2025); historically, earthquakes with M_W up to 5.8 have been recorded in the Basaltic Plateau (Baxter et al., 2021), placing the area at lower end for potential surface rupture and fault scarp development (e.g., Muir et al., 2023). Additionally, contemporary changes in surface strain-rate regime in Uruguay have been documented as a response to the 2010 M_W 8.8 Maule and the 2015 M_W 8.3 Illapel earthquakes in the Andes (Baxter & Smith, 2020).

Moreover, unlike arid locations in the Atacama Desert, Mongolia and Namibia, where climate conditions can preserve fault scarps for tens of millions of years (Muir et al., 2023), the humid subtropical climate of Uruguay promotes intense chemical weathering (Garzanti et al., 2021), therefore shortening the preservation time of the surface expression of faults (Li et al., 2021; Reitman et al., 2019).

Mapped fault scarps on the Basaltic Plateau have slopes of ∼3°–20° (Figures S4 and S5 in Supporting Information S1), consistent with notable degradation of the original escarpment geometry (Avouac, 1993). However, the spatial overlap between recent seismic events and major lineaments suggests that some structures may still be active (Sánchez Bettucci et al., 2025). Therefore, while it is difficult to precisely constrain the timing of deformation in NW Uruguay based on terrain features, the topographic preservation of potential fault scarps under a humid climate points to relatively recent activity.

5.4. Structural Inheritance

Cenozoic deformation structures (potentially including recent features) in the Basaltic Plateau exhibit predominantly NW-SE and ENE-WSW orientations, strongly matching the trends of ancient basement structures mapped across the region (Figure 2; Núñez Demarco et al., 2020). The consistent orientation between recent (this study), post-rift (Cenozoic) (Blanco et al., 2021; Marmisolle et al., 2025; Veroslavsky et al., 2021, 2024), and Mesozoic to Proterozoic (Milani & De Wit, 2008; Núñez Demarco et al., 2020; Oriolo et al., 2018; Passarelli et al., 2011) structures strongly suggests the reactivation of pre-existing structures in NW Uruguay, highlighting the importance of structural inheritance in controlling post-breakup intraplate deformation.

These findings are supported by regional geological and geophysical studies in the area, which link the development of NW-SE-striking lineaments to Proterozoic Pan-African (NE-SW) and late Paleozoic to early Mesozoic Gondwanic (NW-SE) tectonic cycles (Figure 2d; Hueck et al., 2017; Milani & De Wit, 2008; Núñez Demarco et al., 2020; Passarelli et al., 2011; Scherer et al., 2023; Veroslavsky et al., 2021, 2024). Additionally, structural reactivation is also documented in regions adjacent to the Basaltic Plateau, including examples from offshore Uruguay, where ancient NW-SE-structures control the formation of post-rifting depocenters (Marmisolle et al., 2025), as well as further northwest, in Argentina (Mira Carrión et al., 2016). Collectively, these findings

indicate that NW-SE and ENE-WSW-striking structures are regionally significant across the Parana Basin in Uruguay (Veroslavsky et al., 2019, 2021, 2024) and Brazil (Milani & De Wit, 2008; Scherer et al., 2023), and potentially across South America (Veroslavsky et al., 2021).

Our findings are in agreement with post-breakup tectonic reactivation in other sections of the South American passive margin near the south Atlantic Coast in south Brazil (Salomon, Koehn, Passchier, Hackspacher, & Glasmacher, 2015). In this region, volcanic deposits display NNE-SSW-striking deformational features compatible with the orientation of underlying shear zones in the area (Salomon, Koehn, Passchier, Hackspacher, & Glasmacher, 2015). Across the South Atlantic, in Namibia, corresponding Etendeka flows feature similar post-breakup deformation patterns associated with the reactivation of preexisting shear zones (Muir et al., 2023; Salomon, Koehn & Passchier, 2015, Salomon, Koehn, Passchier, Hackspacher & Glasmacher, 2015). These examples highlight the importance of inherited structures in localizing strain and accommodating tectonic reactivation in tectonically "inactive" intraplate settings.

Based on earthquake compilations, notable onshore earthquakes in Uruguay tend to concentrate along major lineaments, particularly the Sarandí del Yí Lineament (Figure 1a; Sánchez Bettucci et al., 2025). Although these earthquakes are relatively infrequent, their occurrence within the Uruguayan Shield highlights the reactivation potential of major crustal lineaments such as those observed across the Basaltic Plateau (Sánchez Bettucci et al., 2025). This ongoing seismic activity indicates that inherited structures may remain mechanically weak and prone to reactivation under the current stress regime (Baxter & Smith, 2020; Sánchez Bettucci et al., 2025).

5.5. Intraplate Tectonics and Landscape Evolution

The long-lived effects of crustal-scale structures, such as lithospheric scars and shear zones, are known to control not only tectonic patterns (Heron et al., 2016) but also reactivation in otherwise "passive" settings (e.g., Rimando & Peace, 2021). Located at the margin of a major ancient Gondwanan structural zone, the Basaltic Plateau exhibits a prolonged history of tectonic reactivation, encompassing structures that date back to the Proterozoic (Oriolo et al., 2015, 2018; Passarelli et al., 2011). Our analysis, combined with data from the literature, reveals that these ancient structural features continue to control surface expressions up to the present via reactivation. In the field, reactivated structures play a key role in concentrating deformation, leading to extensively fractured bedrock (Figure 9). This process is evidenced by the strong match between lineaments and stream orientation (Figure 2), suggesting a correlation between fault damage and erodibility (e.g., Kirkpatrick et al., 2020).

Although planform and hillslope provide evidence of strike-slip deformation (e.g., offset channels and faceted spurs; Figure 5), definitive indicators are sometimes ambiguous or absent along many sections of the potential fault traces. Furthermore, topography may not reliably reflect the current stress field in regions of structural reactivation. This is because deformation tends to localize along pre-existing zones of weakness, favoring the reactivation of inherited structures rather than the formation of new structures (Zhou et al., 2013). Consequently, neotectonic interpretations based solely on surface morphology can be misleading as deformation will be concentrated along pre-existing fault zones (e.g., Rimando & Peace, 2021).

6. Conclusions

In this study we examine topographic, drainage and field data in the Basaltic Plateau in NW Uruguay to determine whether post-breakup tectonics is present in this region. Based on remote and field observations, we conclude that:

- Despite being located in an intraplate setting, geomorphologic evidence suggests post-breakup (Late Cretaceous - Cenozoic) deformation in the Basaltic Plateau, including recent deformation.
- Deformation (fault scarps and offset channels) in the Basaltic Plateau is concentrated along major lineaments, particularly along the Lunarejo, Arroyo Las Cañas, and Sarandí del Yí Lineaments (Figures 5–7).
- Deformation is predominantly accommodated strike-slip faulting, in agreement with modern stress regimes (Baxter & Smith, 2020). Normal faulting is also compatible with stress regime for most of the Cenozoic (Salomon et al., 2015) and potentially with Paleocene–Eocene extensive to neutral condition in the Andean convergence (Horton, 2018).
- Topographic lineaments follow two preferential trends, NW-SE and ENE-WSW (Figure 2). Lineaments largely match the orientation of pre-existing basement structures developed during the Proterozoic Pan-

African (NE-SW) and late Paleozoic to early Mesozoic Gondwanic (NW-SE) tectonic cycles (Milani & De Wit, 2008; Passarelli et al., 2011; Veroslavsky et al., 2021).

- Lineaments have a strong control on drainage pattern and orientation, indicating fault damage control on erodibility (Kirkpatrick et al., 2020). Rivers tend to develop along regional lineaments, which feature extensively fractured bedrock at an outcrop scale (Figure 9).

Conflict of Interest

The authors declare no conflicts of interest relevant to this study.

Data Availability Statement

The medium-resolution (12.5 m/pixel) topographic data used to produce regional analyzes is publicly available at https://asf.alaska.edu (JAXA, 2014), while the high-resolution data is publicly available at https://visualizador.ide.uy/ideuy/core/load_public_project/ideuy (IDEuy, 2018). Geological maps used in this study are publicly available at https://visualizadorgeominero.dinamige.gub.uy/accesos/acceso.html (DINAMIGE, 2017). All mapping was conducted with ArcGIS Pro, while river extraction and analysis was conducted using TopoToolbox 2.3 (Schwanghart & Scherler, 2014) implemented in MATLAB R2021b licensed to LMS. UAV image processing was achieved with Agisoft Metashape. Data collection in the field was conducted using FieldMOVE (https://www.petex.com/pe-geology/move-suite/digital-field-mapping), while structural data was processed using Stereonet 11 (Cardozo & Allmendinger, 2013). Original field data is reported in Tables S1–S3 in Supporting Information S1.

Acknowledgments
We thank Laura Giambiagi, Sebastián Oriolo, and one anonymous reviewer for comments that improved the manuscript, and Josh Wolpert for assistance during fieldwork.

References

Amarante, F. B., Scherer, C. M. S., Goso Aguilar, C. A., Reis, A. D. dos, Mesa, V., & Soto, M. (2019). Fluvial-eolian deposits of the Tacuarembó formation (Norte basin–Uruguay): Depositional models and stratigraphic succession. *Journal of South American Earth Sciences*, *90*, 355–376. https://doi.org/10.1016/j.jsames.2018.12.024

Arioni, L., Velasco Herrera, V. M., Cappellotto, L., Orgeira, M. J., Prezzi, C., & Rossello, E. A. (2024). Seismic forecasting by gapped wavelet transform for the Río de la Plata craton and adjacent continental platform. *Journal of South American Earth Sciences*, *145*, 105069. https://doi.org/10.1016/j.jsames.2024.105069

Avouac, J. (1993). Analysis of scarp profiles: Evaluation of errors in morphologic dating. *Journal of Geophysical Research*, *98*(B4), 6745–6754. https://doi.org/10.1029/92jb01962

Bamberg, B., Reichow, M. K., Walker, R. J., & Ougier-Simonin, A. (2023). Petrological evolution and mass redistribution in basaltic fault zones: An example from the Faroe Islands, North Atlantic igneous province. *Geochemistry, Geophysics, Geosystems*, *24*(12), e2023GC011112. https://doi.org/10.1029/2023gc011112

Baxter, P., Bettucci, L. S., & Costa, C. H. (2021). Assessing the earthquake hazard around the Río de la Plata estuary (Argentina and Uruguay): Implications for risk assessment. *Journal of South American Earth Sciences*, *112*, 103509. https://doi.org/10.1016/j.jsames.2021.103509

Baxter, P., & Smith, E. G. C. (2020). The contemporary strain rate field in Uruguay and surrounding region and possible implications for seismic hazard. *Journal of South American Earth Sciences*, *103*, 102748. https://doi.org/10.1016/j.jsames.2020.102748

Bertin, D., Bustos, E., Grosse, P., & Báez, W. (2025). The central Andes of South America: A review of its tectono-magmatic evolution. *Journal of South American Earth Sciences*, *158*, 105503. https://doi.org/10.1016/j.jsames.2025.105503

Blanco, G., Abre, P., Ferrizo, H., Gaye, M., Gamazo, P., Ramos, J., et al. (2021). Revealing weathering, diagenetic and provenance evolution using petrography and geochemistry: A case of study from the Cretaceous to Cenozoic sedimentary record of the SE Chaco-Paraná basin in Uruguay. *Journal of South American Earth Sciences*, *105*, 102974. https://doi.org/10.1016/j.jsames.2020.102974

Braden, Z., & Behr, W. M. (2021). Weakening mechanisms in a basalt-hosted subduction megathrust fault segment, Southern Alaska. *Journal of Geophysical Research: Solid Earth*, *126*(9), e2021JB022039. https://doi.org/10.1029/2021jb022039

Cardozo, N., & Allmendinger, R. W. (2013). Spherical projections with OSXStereonet. *Computers & Geosciences*, *51*, 193–205. https://doi.org/10.1016/j.cageo.2012.07.021

Cobbold, P. R., Rossello, E. A., Roperch, P., Arriagada, C., Gómez, L. A., & Lima, C. (2007). Distribution, timing, and causes of Andean deformation across South America. *Science Progress*, *272*(1), 321–343. https://doi.org/10.1144/gsl.sp.2007.272.01.17

de Santa Ana, H. (1989). Consideraciones tectonicas y deposicionales de la Cuenca Norte Uruguaya. *Boletín Tecnico de ARPEL*, *18*(4), 319–339.

de Santa Ana, H., & Veroslavsky, G. (2003). La tectosecuencia volcanosedimentaria de la Cuenca Norte de Uruguay. Edad Jurásico-Cretácico Temprano. In G. Veroslavsky, M. Ubilla, & S. Martínez (Eds.), *Cuencas Sedimentarias de Uruguay: Geología, Paleontología y Recursos Naturales*. Mesozoico. DI.R.A.C.

Dirección Nacional de Minería y Geología (DINAMIGE). (2017). Carta Geológica del Uruguay digital a escala 1.500.000 [Dataset]. Retrieved from https://visualizadorgeominero.dinamige.gub.uy/accesos/acceso.html

dos Santos, J. M., Salamuni, E., da Silva, C. L., Sanches, E., Gimenez, V. B., & do Nascimento, E. R. (2019). Morphotectonics in the central-east region of south Brazil: Implications for catchments of the lava-tudo and Pelotas Rivers, State of Santa Catarina. *Geomorphology*, *328*, 138–156. https://doi.org/10.1016/j.geomorph.2018.12.016

Duvall, A. R., & Tucker, G. E. (2015). Dynamic ridges and valleys in a strike-slip environment. *Journal of Geophysical Research: Earth Surface*, *120*(10), 2016–2026. https://doi.org/10.1002/2015jf003618

Fontainha, M. V. F., Trouw, R. A. J., Dantas, E. L., Polo, H. J. O., Serafim, I. C. C. O., Furtado, P. C., & Negrão, A. P. (2021). Reactivated shear zones: A case study in a tectonic superposition zone between the southern Brasília and Ribeira orogens, southeastern Brazil. *Journal of South American Earth Sciences*, *112*, 103537. https://doi.org/10.1016/j.jsames.2021.103537

Garzanti, E., Dinis, P., Vezzoli, G., & Borromeo, L. (2021). Sand and mud generation from continental flood basalts in contrasting landscapes and climatic conditions (Paraná–Etendeka conjugate igneous provinces, Uruguay and Namibia). *Sedimentology*, *68*(7), 3447–3475. https://doi.org/10.1111/sed.12905

Giona Bucci, M., & Schoenbohm, L. M. (2022). Tectono-geomorphic analysis in low relief, low tectonic activity areas: Case study of the temiskaming region in the Western Quebec seismic zone (WQSZ), Eastern Canada. *Remote Sensing*, *14*(15), 3587. https://doi.org/10.3390/rs14153587

Gomes, A. S., & Vasconcelos, P. M. (2021). Geochronology of the Paraná-Etendeka large igneous province. *Earth-Science Reviews*, *220*, 103716. https://doi.org/10.1016/j.earscirev.2021.103716

Heron, P. J., Pysklywec, R. N., & Stephenson, R. (2016). Lasting mantle scars lead to perennial plate tectonics. *Nature Communications*, *7*(1), 11834. https://doi.org/10.1038/ncomms11834

Horton, B. K. (2018). Tectonic regimes of the central and Southern andes: Responses to variations in plate coupling during subduction. *Tectonics*, *37*(2), 402–429. https://doi.org/10.1002/2017tc004624

Hueck, M., Oriolo, S., Dunkl, I., Wemmer, K., Oyhantçabal, P., Schanofski, M., et al. (2017). Phanerozoic low-temperature evolution of the Uruguayan shield along the South American passive margin. *Journal of the Geological Society*, *174*(4), 609–626. https://doi.org/10.1144/jgs2016-101

Instituto Nacional de Estadística, Ministerio de Transporte y Obras Públicas, Dirección Nacional de Topografía (IDEuy). (2018). Relieve (IDEuy) [Dataset]. Retrieved from https://visualizador.ide.uy/ideuy/core/load_public_project/ideuy/

JAXA, M. E. T. I. (2014). ALOS PALSAR, radiometrically and terrain-corrected digital elevation model [Dataset]. Retrieved from https://asf.alaska.edu

Karson, J. A., Farrell, J. A., Chutas, L. A., Nanfito, A. F., Proett, J. A., Runnals, K. T., & Sæmundsson, K. (2018). Rift-parallel strike-slip faulting near the Iceland plate boundary zone: Implications for propagating rifts. *Tectonics*, *37*(12), 4567–4594. https://doi.org/10.1029/2018tc005206

Kirkpatrick, H. M., Moon, S., Yin, A., & Harrison, T. M. (2020). Impact of fault damage on eastern Tibet topography. *Geology*, *49*(1), 30–34. https://doi.org/10.1130/g48179.1

Kröhling, D., Brunetto, E., Galina, G., Zalazar, M. C., & Iriondo, M. (2014). Planation surfaces on the Paraná basaltic Plateau, South America. *Gondwana Landscapes in southern South America*. https://doi.org/10.1007/978-94-007-7702-6_10

Li, X., Pierce, I. K. D., Ai, M., Luo, Q., Li, C., Zheng, W., & Zhang, P. (2022). Active tectonics and landform evolution in the Longxian-Baoji fault zone, Northeast Tibet, China, determined using combined ridge and stream profiles. *Geomorphology*, *410*, 108279. https://doi.org/10.1016/j.geomorph.2022.108279

Li, Y., Liu, M., Zhang, H., & Shi, Y. (2021). Stream channel offsets along strike-slip faults: Interaction between fault slip and surface processes. *Geomorphology*, *394*, 107965. https://doi.org/10.1016/j.geomorph.2021.107965

Manna, M. O., Santos Scherer, C. M. dos, Bállico, M. B., Goso, C. A., Kifumbi, C., Schaffer, G., et al. (2025). Paleoenvironmental reconstruction and stratigraphic implications of the middle to late Permian yaguarí formation, norte basin, Uruguay. *Journal of South American Earth Sciences*. https://doi.org/10.1016/j.jsames.2025.105381

Marmisolle, J., Morales, E., Rossello, E., Soto, M., & Hernández-Molina, J. (2025). Tectonic evolution of the Atlantic rift, central sector offshore Uruguay. *Tectonophysics*, *899*, 230654. https://doi.org/10.1016/j.tecto.2025.230654

Marmisolle, J., Veroslavsky, G., & de Santa Ana, H. (2016). Depocenters with potential preservation of pre-carboniferous rocks in norte Basin (Uruguay). In *International conference and exhibition* (pp. 18–20). https://doi.org/10.1190/ice2016-6337268.1

Milani, E. J., & De Wit, M. J. (2008). Correlations between the classic Paraná and Cape–Karoo sequences of South America and southern Africa and their basin infills flanking the Gondwanides: Du Toit revisited. *Science Progress*, *294*(1), 319–342. https://doi.org/10.1144/sp294.17

Mira Carrión, A., Veroslavsky, G., Vives, L., & Rodríguez, L. (2016). Influencia de los lineamientos estructurales sobre el flujo del Sistema Acuífero Guaraní en la provincia de Corrientes. *Revista de la Asociación Geológica Argentina*, *73*(4), 478–492.

Moon, S., Perron, J. T., Martel, S. J., Holbrook, W. S., & St. Clair, J. (2017). A model of three-dimensional topographic stresses with implications for bedrock fractures, surface processes, and landscape evolution. *Journal of Geophysical Research: Earth Surface*, *122*(4), 823–846. https://doi.org/10.1002/2016jf004155

Morales, E., Veroslavsky, G., Manganelli, A., Marmisolle, J., Pedro, A., Samaniego, L., et al. (2021). Potential of geothermal energy in the onshore sedimentary basins of Uruguay. *Geothermics*, *95*, 102165. https://doi.org/10.1016/j.geothermics.2021.102165

Muir, R. A., Whitehead, B. A., New, T., Stevens, V., Macey, P. H., Groenewald, C. A., et al. (2023). Exceptional scarp preservation in SW Namibia reveals geological controls on large magnitude intraplate seismicity in Southern Africa. *Tectonics*, *42*(4), e2022TC007693. https://doi.org/10.1029/2022tc007693

Muzio, R., Olivera, L., Fort, S., & Peel, E. (2022). Petrological features of the first Cenozoic alkaline magmatic event recorded in northwestern Uruguay, southern extreme of the Paraná basin. *Journal of South American Earth Sciences*, *116*, 103796. https://doi.org/10.1016/j.jsames.2022.103796

Núñez Demarco, P., Masquelin, H., Prezzi, C., Aïfa, T., Muzio, R., Loureiro, J., et al. (2020). Aeromagnetic patterns in Southern Uruguay: Precambrian-mesozoic dyke swarms and Mesozoic rifting structural and tectonic evolution. *Tectonophysics*. https://doi.org/10.1016/j.tecto.2020.228373

Oriolo, S., Hueck, M., Oyhantçabal, P., Goscombe, B., Wemmer, K., & Siegesmund, S. (2018). Shear zones in brasiliano-pan-african belts and their role in the amalgamation and Break-Up of Southwest gondwana. *Regional Geology Reviews*, 593–613. https://doi.org/10.1007/978-3-319-68920-3_22

Oriolo, S., Oyhantçabal, P., Basei, M. A. S., Wemmer, K., & Siegesmund, S. (2016). The Nico Pérez Terrane (Uruguay): From Archean crustal growth and connections with the Congo Craton to late Neoproterozoic accretion to the Río de la Plata Craton. *Precambrian Research*, *280*, 147–160. https://doi.org/10.1016/j.precamres.2016.04.014

Oriolo, S., Oyhantçabal, P., Heidelbach, F., Wemmer, K., & Siegesmund, S. (2015). Structural evolution of the Sarandí del Yí Shear Zone, Uruguay: Kinematics, deformation conditions and tectonic significance. *International Journal of Earth Sciences*. https://doi.org/10.1007/s00531-015-1166-2

Panara, Y., Menegoni, N., Finkbeiner, T., Zühlke, R., & Vahrenkamp, V. (2024). High-resolution analysis of 3D fracture networks from digital outcrop models, correlation to plate-tectonic events and calibration of subsurface models (Jurassic, Arabian plate). *Marine and Petroleum Geology*, *167*, 106998. https://doi.org/10.1016/j.marpetgeo.2024.106998

Panario, D., Gutiérrez, O., Sánchez Bettucci, L., Peel, E., Oyhantçabal, P., & Rabassa, J. (2014). Ancient landscapes of Uruguay. *Gondwana Landscapes in southern South America*, 161–199. https://doi.org/10.1007/978-94-007-7702-6_8

Pascal, C. (2022). Brittle structures in the field. *Paleostress Inversion Techniques*, 3–24. https://doi.org/10.1016/b978-0-12-811910-5.00006-3

Passarelli, C. R., Basei, M. A. S., Wemmer, K., Siga, O., Jr., & Oyhantçabal, P. (2011). Major shear zones of southern Brazil and Uruguay: Escape tectonics in the eastern border of Rio de La plata and Paranápanema cratons during the Western Gondwana amalgamation. *International Journal of Earth Sciences*, *100*(2–3), 391–414. https://doi.org/10.1007/s00531-010-0594-2

Peace, A. L., & Jess, S. (2023). Microdrones in field-based structural geology: A photogrammetry and fracture quantification case study from the North Mountain basalt, Nova Scotia, Canada. *Drone System Application*, *11*, 1–15. https://doi.org/10.1139/dsa-2022-0037

Pereira-Claren, A., Gironás, J., Niemann, J. D., Passalacqua, P., Mejia, A., & Escauriaza, C. (2019). Planform geometry and relief characterization of drainage networks in high-relief environments: An analysis of Chilean Andean basins. *Geomorphology*, *341*, 46–64. https://doi.org/10.1016/j.geomorph.2019.05.011

Preciozzi, F., Spoturno, J., Rossi, P., & Heinzen, W. (1985). *Carta geológica del Uruguay a escala 1: 500.000 y Memoria Explicativa. Ministerio de Industria, Energía y Minería*. Dirección Nacional de Minería y Geología.

Reitman, N. G., Mueller, K. J., Tucker, G. E., Gold, R. D., Briggs, R. W., & Barnhart, K. R. (2019). Offset channels may not accurately record strike-slip fault displacement: Evidence from landscape evolution models. *Journal of Geophysical Research: Solid Earth*, *124*(12), 13427–13451. https://doi.org/10.1029/2019jb018596

Rimando, J. M., & Peace, A. L. (2021). Reactivation potential of intraplate faults in the Western Quebec seismic zone, Eastern Canada. *Earth and Space Science*, *8*(8), e2021EA001825. https://doi.org/10.1029/2021ea001825

Rodríguez, P., Marmisolle, J., Soto, M., Gristo, P., Benvenuto, A., de Santa Ana, H., & Veroslavsky, G. (2015). *Preliminary results of new gravity surveys onshore Uruguay, with a 2D modeling case study from Norte basin*. SEG Technical Program Expanded Abstracts. https://doi.org/10.1190/segam2015-5814479.1

Rodríguez, P., Veroslavsky, G., Soto, M., Marmisolle, J., Gristo, P., de Santa Ana, H., & Benvenuto, A. (2015). New integrated Bouguer gravity anomaly map onshore Uruguay: Preliminary implications for the recognition of crustal domains. *SEG Technical Program Expanded Abstracts*, 1515–1519. https://doi.org/10.1190/segam2015-5821993.1

Salamuni, E., da Silva, C. L., do Nascimento, E. R., dos Santos, J. M., Peyerl, W. R. L., & Gimenez, V. B. (2021). Morphometric and structural diagnosis of fault reactivation in the Cenozoic: A case study of the Blumenau-Soledade Lineament in southern Brazil. *Brazilian Journal of Genetics*, *51*(3), e20200080. https://doi.org/10.1590/2317-4889202120200080

Salomon, E., Koehn, D., & Passchier, C. (2015). Brittle reactivation of ductile shear zones in NW Namibia in relation to South Atlantic rifting. *Tectonics*, *34*(1), 70–85. https://doi.org/10.1002/2014tc003728

Salomon, E., Koehn, D., Passchier, C., Hackspacher, P. C., & Glasmacher, U. A. (2015). Contrasting stress fields on correlating margins of the South Atlantic. *Gondwana Research*, *28*(3), 1152–1167. https://doi.org/10.1016/j.gr.2014.09.006

Sánchez Bettucci, L., Kacevas, M. R., Castro, H., Olivet, J. L., & Latorres, E. (2025). Summary of the intracontinental seismicity of Uruguay. *Journal of South American Earth Sciences*, *161*, 105578. https://doi.org/10.1016/j.jsames.2025.105578

Scherer, C. M. S., Reis, A. D., Horn, B. L. D., Bertolini, G., Lavina, E. L. C., Kifumbi, C., & Goso Aguilar, C. (2023). The stratigraphic puzzle of the permo-mesozoic southwestern Gondwana: The Paraná basin record in geotectonic and palaeoclimatic context. *Earth-Science Reviews*, *240*, 104397. https://doi.org/10.1016/j.earscirev.2023.104397

Schwanghart, W., & Scherler, D. (2014). Short communication: TopoToolbox 2 – MATLAB-based software for topographic analysis and modeling in Earth surface sciences. *Earth Surface Dynamics*, *2*, 1–7. https://doi.org/10.5194/esurf-2-1-2014

Tibaldi, A., Corti, N., De Beni, E., Bonali, F. L., Falsaperla, S., Langer, H., et al. (2021). Mapping and evaluating kinematics and the stress and strain field at active faults and fissures: A comparison between field and drone data at the NE rift, Mt Etna (Italy). *Solid Earth*, *12*(4), 801–816. https://doi.org/10.5194/se-12-801-2021

Veroslavsky, G., Aubet, N., Martínez, S. A., Heaman, L. M., Cabrera, F., & Mesa, V. (2019). Late Cretaceous stratigraphy of the southeastern Chaco–Paraná basin ("Norte Basin"–Uruguay): The Maastrichtian age of the calcretization process. https://doi.org/10.5016/geociencias.v38i2.13779

Veroslavsky, G., de Santa Ana, H., Goso, C., & Gonzalez, S. (1997). Calcretas y silcretas de la región oeste Uruguay (Queguay), cuenca de Paraná (Cretácico Superior–Terciário Inferior). *Geociencias*, *16*(1), 205–224.

Veroslavsky, G., Rossello, E. A., López-Gamundí, O., de Santa Ana, H., Assine, M. L., Marmisolle, J., & de J Perinotto, A. (2021). Late Paleozoic tectono-sedimentary evolution of eastern Chaco-Paraná basin (Uruguay, Brazil, Argentina and Paraguay). *Journal of South American Earth Sciences*. https://doi.org/10.1016/j.jsames.2020.102991

Veroslavsky, G., Soto, M., Mesa, V., & Manganelli, A. (2024). Geology of the Guaraní aquifer system in the outcrop area of the Tacuarembó and Rivera formations (Norte Basin, Uruguay). *Revista de la Asociación Geológica Argentina*, *81*(2), 239–264.

Walker, R. J., Holdsworth, R. E., Armitage, P. J., & Faulkner, D. R. (2013). Fault zone permeability structure evolution in basalts. *Geology*, *41*(1), 59–62. https://doi.org/10.1130/g33508.1

Woodcock, N. H., & Mort, K. (2008). Classification of fault breccias and related fault rocks. *Geological Magazine*, *145*(3), 435–440. https://doi.org/10.1017/s0016756808004883

Zhou, R., Schoenbohm, L. M., & Cosca, M. (2013). Recent, slow normal and strike-slip faulting in the Pasto Ventura region of the southern Puna Plateau, NW Argentina. *Tectonics*, *32*(1), 19–33. https://doi.org/10.1029/2012tc003189